RESEARCH PAPER

Effects of sonication on the Physical and biological Properties of Carica Papaya and Moringa Oleifera Leafs for biomedical applications

G. Samuel[1], K. Srijanani[1], I. Johnson[1]

[1]Department of Physics, St. Joseph's College (Autonomous), Affiliated to Bharathidasan University, Tiruchirappalli-620 002, Tamilnadu, India.

Corresponding author details:
Dr. G. Samuel
Assistant Professor, Department of Physics
St. Joseph's College (Autonomous), Tiruchirappalli – 620002
E-mail: samuel_ph1@mail.sjctni.edu

ABSTRACT

This study investigates the effects of sonication on the physical and biochemical properties of *Carica papaya* and *Moringa oleifera* leaf extracts, focusing on macromolecule extraction and antimicrobial activity. Key physical parameters, including density, viscosity, ultrasonic velocity, adiabatic compressibility, and acoustic impedance, were measured before and after sonication. Biochemical analyses assessed protein and carbohydrate levels at 5- to 15-minute sonication intervals. Structural changes were evaluated using Fourier-transform infrared (FTIR) and UV spectroscopy, while particle size analysis determined the impact of sonication-induced shear forces. Antimicrobial activity was tested against *Enterococcus faecalis* and *Pseudomonas aeruginosa*. Sonication significantly altered the physical properties of the extracts and progressively increased protein and carbohydrate levels. FTIR and UV analyses confirmed structural changes and cell disruption, evidenced by modifications in peak intensities and functional groups. Particle size analysis revealed a marked reduction due to shear forces and enhanced mass transfer. Antimicrobial assays showed that *Carica papaya* demonstrated a 12 mm zone of inhibition against *Enterococcus faecalis* before sonication but no activity against *Pseudomonas aeruginosa*. Conversely, *Moringa oleifera* exhibited no antimicrobial activity against either strain, irrespective of sonication. Sonication enhances the extraction of macromolecules and induces structural changes in *Carica papaya* and *Moringa oleifera* leaf extracts. While sonication increases biochemical content and antimicrobial potential in *Carica papaya*, *Moringa oleifera* shows limited antibacterial effects regardless of sonication. These findings highlight the potential of sonication for optimizing macromolecule extraction in *Carica papaya*.

Keywords: Sonication; Antimicrobial Activity; *Carica Papaya*; *Moringa Oleifera*; Biochemical Properties; UV Analysis.

How to cite this article: Samuel G, Srijanani K, Johnson I. Effects of sonication on the Physical and biological Properties of Carica Papaya and Moringa Oleifera Leafs for biomedical applications. Int J Drug Deliv Technol. 2026;16(54s): 988-1013. DOI: 10.25258/ijddt.16.54s.87

Source of support: Nil.

Conflict of interest: None.

. Introduction

To discuss the structure of liquids, two fundamental problems must be addressed. First, understanding the nature of molecular interactions is crucial. Recent studies indicate that the forces between molecules are repulsive at small separations and attractive at longer distances, which significantly influence liquid behavior (Prusty et al., 2024) **[1].** Second, the challenge is to relate the bulk or macroscopic properties of a liquid to its microscopic or molecular properties, particularly the potential energy function describing molecular interactions (Riera et al., 2020) **[2]**. Liquids possess properties that fall between those of solids and gases. However, it is not always the case that liquid properties are mere averages of the two. Studies show that the properties of liquids tend to resemble either solids or gases, depending on specific factors, such as molecular arrangement and temperature (Horstmann , 2022) **[3]**. Liquids lack the rigidity seen in solids and, like gases, assume the shape of their container, yet retain some degree of cohesion, much like solids, allowing them to maintain a free surface (Ulusoy et al., 2023) **[4]**.

Both liquids and solids are relatively incompressible compared to gases, with recent data indicating that the compressibility of liquids is about 10^{-5} atm^{-1}, slightly larger than solids but significantly lower than that of gases (Tanasheva et al., 2024) **[5]**. This similarity in compressibility between liquids and solids highlights their comparable densities. In general, the density of liquids decreases only by 10-15% upon melting, whereas vaporization leads to a drastic decrease in density by several orders of magnitude (Zelenski et al., 2021) **[6]**. Consequently, molecular separations in liquids are comparable to those in solids, with minimal free space between molecules, in contrast to the large separations typical in gases (Zhang et al., 2021) **[7]**. Forces between molecules in liquids operate over short ranges, typically affecting only a few molecular diameters. These forces are negligible in gases due to the random movement of molecules but are critical in liquids, where close molecular proximity leads to cohesion (Špadina et al., 2021) **[8]**.

Liquids flow because molecular movement is possible within the close-packed structure, but this movement requires overcoming greater resistance than in gases due to the higher density (Moradpour et al., 2024) [9]. Solids, in contrast, have a highly ordered molecular arrangement that prevents flow under small stresses. This rigidity is accompanied by low potential energy, requiring significant energy input to transition from solid to liquid (Gao et al., 2024) [10]. Liquids, while maintaining some order in their molecular packing, exhibit slight irregularities that differentiate them from solids. Recent models propose that molecular clusters may form temporarily, causing local density fluctuations (Lee et. al., 2021) [11]. The molecular structure of gases is often described by chaotic, free movement of molecules, whereas in liquids, molecular separations are comparable to molecular diameters. The volume occupied by liquids is close to that of their molecules, meaning that intermolecular forces play a substantial role in maintaining liquid density and reducing compressibility (Saini et. al., 2021) [12].

Liquids flow under stress, but this requires molecules to push past each other, leading to greater resistance than seen in gases, where molecules move freely through large empty spaces (Vogel et. al., 2020) [13]. Solids maintain a fixed structure due to the close packing of their molecules, which limits movement under stress. Upon the application of force, solids deform slightly but return to their original shape once the force is removed, demonstrating their rigidity (Hertzberg et al., 2020) [14]. In solids, potential energy is minimized, and substantial energy input is necessary for a phase change into the liquid state (Fu et. al., 2022) [15]. Recent advancements in sonication, which uses high-frequency sound waves, have shown that it can disrupt molecular structures in liquids for applications such as emulsification and biomolecule fragmentation. This technique is increasingly used in pharmaceutical and biochemical industries (Manickam et. al, 2023) [16].

Sonication can fragment biomolecules, an effect that is useful in some contexts but must be controlled to avoid damaging molecular structures crucial for biological function (Hahmann et al., 2024) [17]. Modern techniques for studying molecular interactions in liquids include Nuclear Magnetic Resonance (NMR) and ultrasonic methods. These techniques have advanced significantly, allowing for the detailed investigation of molecular behavior under various conditions. NMR is particularly useful for observing proton-bearing molecules, while ultrasonic methods are effective for probing weak molecular interactions (Li et. al, 2020) [18]. Ultrasonic studies offer a valuable method for measuring physical properties such as density, viscosity, and ultrasonic velocity in liquids (Fan et al., 2021) [19]. These studies provide insight into the molecular interactions at play, making it possible to calculate additional parameters like acoustic impedance and adiabatic compressibility (Das et. al., 2024) [20].

2. Materials and Methods

2.1 Temperature Control and Density Measurement:

A constant temperature bath was employed to maintain the temperature at 308.15 ± 0.01 K, ensuring precise control over experimental conditions. The density of pure liquids, liquid mixtures, and electrolyte solutions was measured using the relative measurement method. A clean, dry 10 ml specific gravity bottle was filled with double-distilled water, which served as the reference liquid, and immersed in the temperature-controlled bath. The water in the bottle was allowed to equilibrate thermally with the bath before the mass (W_2) was measured using an electronic balance with a precision of 0.1 mg. The density of water was calculated using the formula $mw=W_2-W_1$, where W_1 and W_2 represents the mass of the empty bottle. To determine the density of the unknown liquid mixture, the specific gravity bottle was filled with the sample, and its mass was measured under the same experimental conditions. The density was calculated using the same procedure. Reference values for the density of water at different temperatures were obtained from literature sources. This approach ensured high accuracy, with the precision of measurements directly dependent on the electronic balance used.

2.2 Viscosity Measurement Using Oswald Viscometer

The Oswald viscometer was thoroughly cleaned using acetone and dried to ensure accurate measurements. It was then mounted in a constant temperature water bath maintained at 298 K. The liquid under test was introduced into the upper bulb of the viscometer up to the marked level. The time taken for the meniscus to pass between the marks during its free fall was recorded using a stopwatch. This procedure was repeated multiple times for accuracy, and the viscometer was cleaned after each measurement.

2.3 Ultrasonic Velocity Measurement of Liquid Mixtures Using the Interferometer Method

The ultrasonic velocity was measured using an interferometer consisting of a high-frequency generator and a double-walled measuring cell. The cell was designed to circulate water between its inner and outer walls to maintain a constant temperature. A quartz crystal at the bottom of the cell generated longitudinal ultrasonic waves when excited by the generator. A reflector plate was adjusted vertically using a micrometer screw, and standing waves were formed when the distance between the reflector and the crystal matched an integral multiple of half the wavelength. The maximum anode current corresponding to the resonance condition was measured, and the velocity of the ultrasonic waves in the mixture was calculated using the formula $v=2dn$, where d is the distance moved by the reflector and ν is the frequency of the generator.

2.4 Sonication for Bioactive Compound Extraction from Carica Papaya and Moringa Oleifera Leaves

Leaves of Carica Papaya and Moringa Oleifera (**Fig.1**) were separated and boiled in distilled water for 30 minutes. The extracts were then filtered using filter paper and divided into two beakers (A and B). Beaker A remained undisturbed, while Beaker B was subjected to sonication for 5 and 15 minutes (**Fig.2**), respectively, to enhance the extraction process. Density measurements were performed using a relative density bottle, viscosity was assessed with an Oswald viscometer, and ultrasonic velocity was measured using an ultrasonic interferometer for both samples. **Table 1** lists the Physical properties of Carica Papaya leaf and **Table 2** lists physical properties of moringa oleifera leaf.

2.5 Preparation and Incubation of Microbial Inoculum for Antimicrobial Testing

Stock cultures of the test microorganisms were maintained on nutrient agar slants at 4°C. A loopful of cells was transferred from the stock culture to test tubes containing nutrient broth, which were then incubated for 24 hours at 37ºC to prepare the active cultures. The antimicrobial activity was assessed using the agar well diffusion method to determine the efficacy of the extracts.

3. RESULT AND DISCUSSION with CHARACTERIZATION TECHNIQUES

RESULTS AND DISCUSSION

5.1. PHYSICAL PROPERTIES OF THE SAMPLES:

5.1.1. PHYSICAL PROPERTIES OF CARICA PAPYA LEAF:

PHYSICAL PROPERTIES	BEFORE SONICATION	AFTER SONICATION (5 MINUTES)	AFTER SONICATION (15 MINUTES)
DENSITY(ρ) ($\frac{kg}{m^3}$)	1004	1766.3656	1765.6587
VISCOSITY(η) (NSm^2)	0.8170	1.5477	1.4831
ULTRA SONIC VELOCITY(U) ($\frac{m}{s}$)	1520	1419	1542
ADIABATIC COMPRESSIBILITY x 10^{-10}x(β)x($\frac{m^2}{N}$)	4.3433	2.8177	3.3797
ACOUSTIC IMPEDANCE X 10^6x (Z) x ($\frac{kg^2}{m^2 Xs}$)	1.526	2.508	2.723

Table.5.1.1

5.1.2. PHYSICAL PROPERTIES OF MORINGA OLEIFERA LEAF:

PHYSICAL PROPERTIES	BEFORE SONICATION	AFTER SONICATION (5 MINUTES)	AFTER SONICATION (15 MINUTES)
DENSITY(ρ) ($\frac{kg}{m^3}$)	**1002.8277**	**1767.4616**	**1763.3915**
VISCOSITY(η) (NSm^2)	**0.7961**	**1.4330**	**1.4541**
ULTRA SONIC VELOCITY(U) ($\frac{m}{s}$)	**1469**	**1324**	**1478**
ADIABATIC COMPRESSIBILITY x 10^{-10}x(β)x($\frac{m}{N}$)^2	**4.6249**	**2.5906**	**3.2357**
ACOUSTIC IMPEDANCE X 10^6x (Z) x ($\frac{kg}{m^2XS}$)^2	**1.4732**	**2.6135**	**2.3349**

able.5.1.2

- From the physical properties of both papaya and moringa leaves shows that interval between before sonication and after sonication (5 Minutes) of Density,Viscosity there is an initial increase could be due to the breakdown of cellular structures and the release of intracellular compounds such as proteins.
- Decreased at 15 minutes of sonication may lead to further breakdown of cell walls and components causing more release of intracellular materials and gases.
-
- It indicates that most of the significant changes occurred within the first 5 minutes.

5.2. PROTEIN ESTIMATION:

5.2.1. CARICA PAPAYA LEAF:5.2.2 MORINGA OLEIFERA LEAF:

TIME INTERVAL	AMOUNT OF PROTEIN(µg)
Before Sonication	300
5 minutes	330
15 minutes	440

TIME INTERVAL	AMOUNT OF PROTEIN(µg)
Before Sonication	610
5 minutes	630
15 minutes	740

Table.5.2.1Table.5.2.2

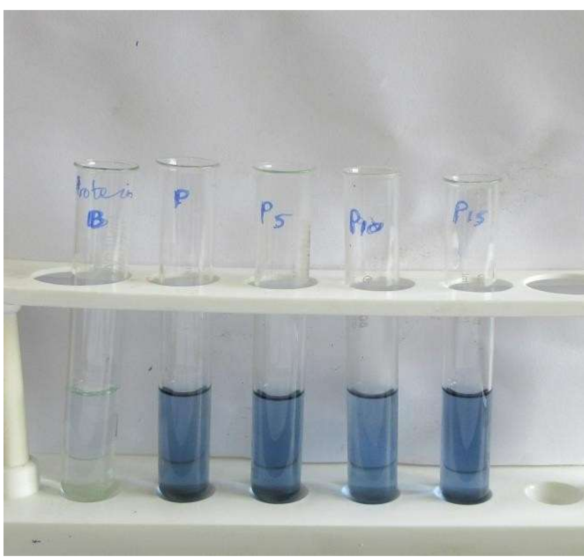

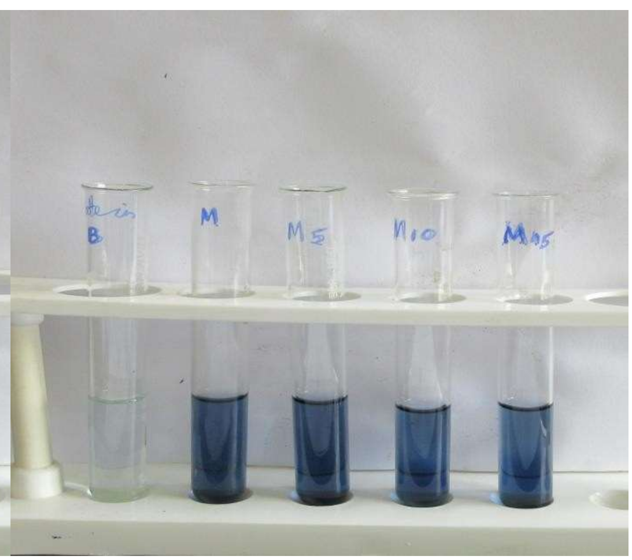

Fig.5.2.1 **Fig.5.2.2**

The Protein Estimation of Carica Papaya and MoringaOleifera Leaves before sonication and after sonication for the time intervals of 5 minutes and 15 minutes was observed and it confirms that there is an gradual increasing in the estimation of Protein after sonication.

5.3 CARBOHYDRATE ESTIMATION:

5.3.1. CARICA PAPAYA LEAF:

Table.5.3.1

TIME INTERVAL	AMOUNT OF CARBOHYDRATE(μg)
Before Sonication	170
5 minutes	200
15 minutes	340

5.3.2 MORINGA OLEIFERA LEAF:

Table.5.3.2

TIME INTERVAL	AMOUNT OF CARBOHYDRATE(μg)
Before Sonication	280
5 minutes	270
15 minutes	300

The Carbohydrate Estimation of Carica Papaya and MoringaOleifera Leaves before sonication and after sonication for the time intervals of 5 minutes and 15 minutes was observed and it confirms that there is an gradual increasing in the estimation of Carbohydrate after sonication.

5.4. ULTRAVIOLET SPECTROSCOPY(UV) :

5.4.1. CARICA PAPAYA LEAF:

UV BEFORE SONICATION :

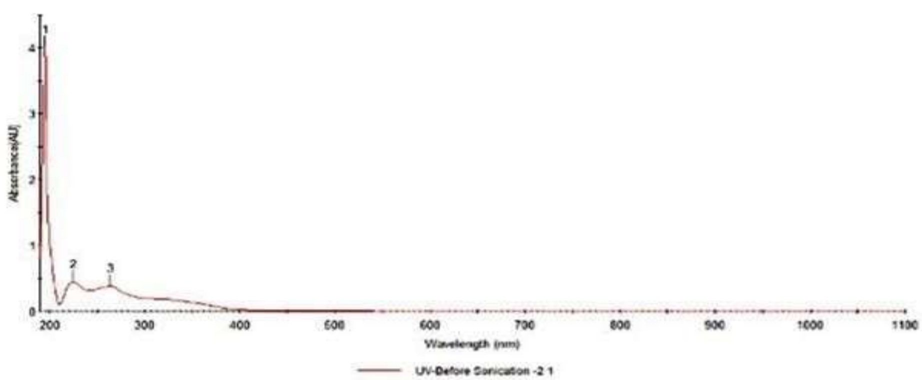

Name	No.	Peak(nm)	Peak(AU)	No.	Valley(nm)	Valley(AU)
UV-Before Sonication -	1	195.2	4.00			
	2	225.5	0.45			
	3	263.8	0.39			

Graph.5.4.1.1

UV AFTER SONICATION **UV AFTER SONICATION (5 MINUTES): (15 MINUTES):**

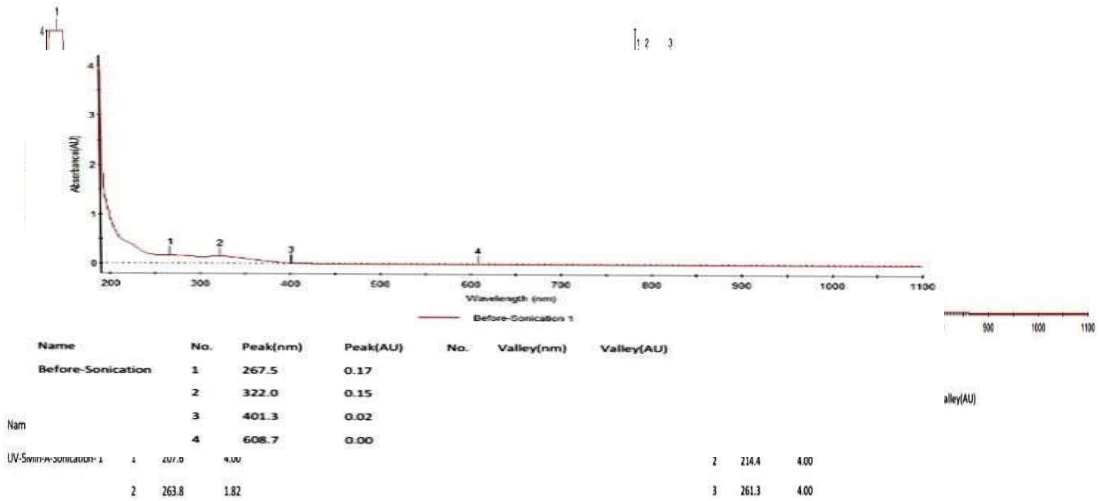

Name	No.	Peak(nm)	Peak(AU)	No.	Valley(nm)	Valley(AU)
Before-Sonication	1	267.5	0.17			
	2	322.0	0.15			
	3	401.3	0.02			
	4	608.7	0.00			

UV-5min-A-sonication- 1	1	207.6	4.00
	2	263.8	1.82

2	214.4	4.00
3	261.3	4.00

Graph.5.4.1.2 Graph.5.4.1.3

5.4.2. MORINGA OLEIFERA LEAF: UV BEFORE SONICATION :

Graph.5.4.2.1

UV AFTER SONICATION **UV AFTER SONICATION (5 MINUTES): (15 MINUTES):**

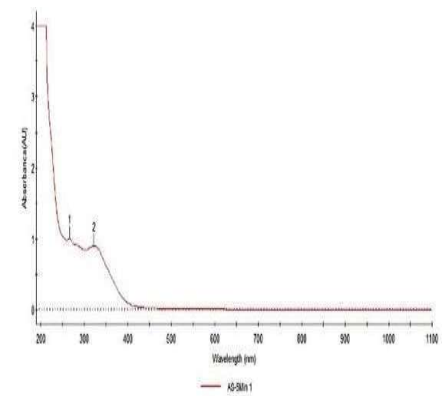

Name	No.	Peak(nm)	Peak(AU)	No.	Valley(nm)	Valley(AU)
AS-5Min	1	266.3	1.00			
	2	322.0	0.90			

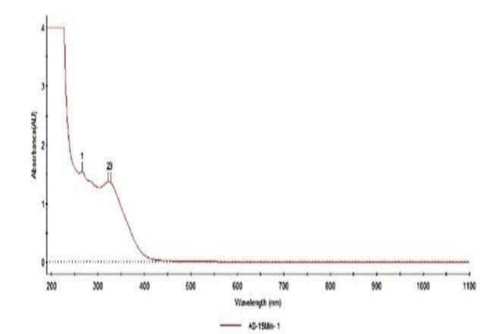

Name	No.	Peak(nm)	Peak(AU)	No.	Valley(nm)	Valley(AU)
AS-15Min-	1	266.3	1.54			
	2	322.0	1.38			
	3	327.0	1.37			

Graph.5.4.2.2

Graph.5.4.2.3

5.5 PARTICLE SIZE ANANLYSER:

5.5.1. CARICA PAPAYA LEAF :

PSA BEFORE SONICATION:

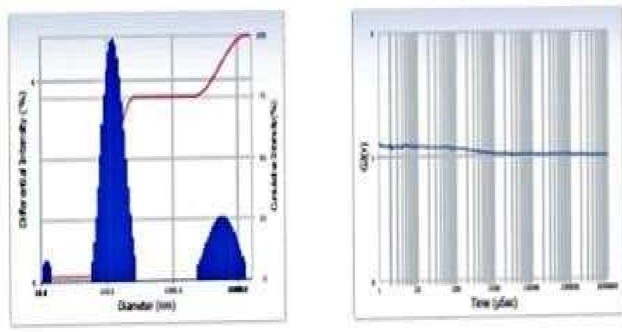

DIAMETER(d)-693.2(nm)

Fig.5.5.1.1

PSA AFTER SONICATION

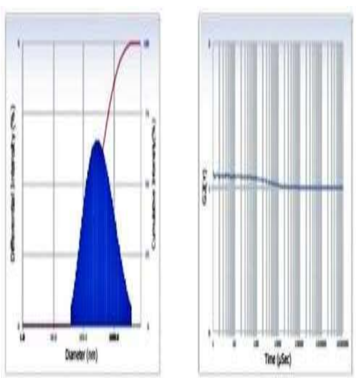

DIAMETER(d)-367(nm)

Fig.5.5.1.2

PSA AFTER SONICATION (5 MINUTES):
(15 MINUTES):

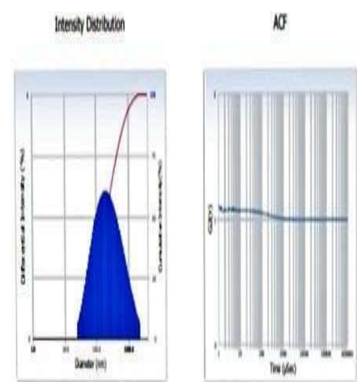

DIAMETER(d)-178.9(nm)

Fig.5.5.1.3

5.5.2. MORINGA OLEIFERA LEAF: PSA BEFORE SONICATION:

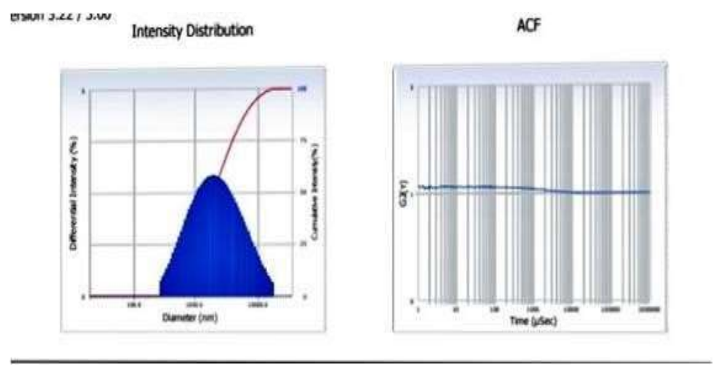

DIAMETER(d)-1494.4(nm)
Fig.5.5.2.1

PSA AFTER SONICATION

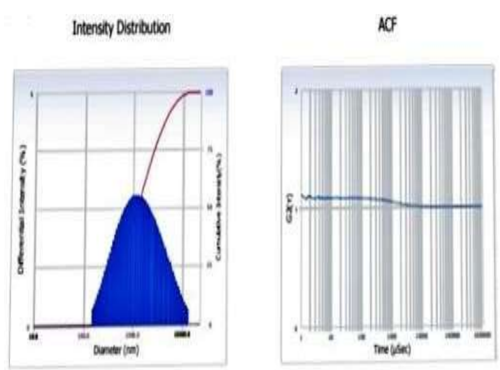

DIAMETER(d)-1305.6 (nm)
Fig.5.5.2.2

PSA AFTER SONICATION (5 MINUTES):
(15 MINUTES):

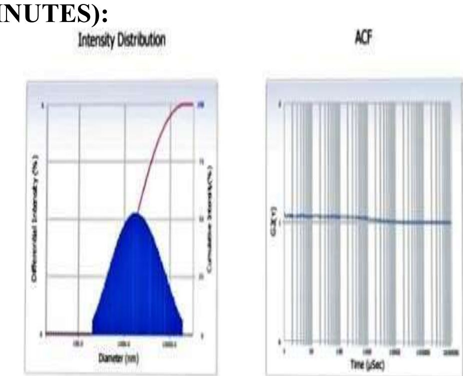

DIAMETER(d)-1002.4(nm)
Fig.5.5.2.3

5.6 FOURIER TRANSFORM INFRARED SPECTROSCOPY:

5.6.1. CARICA PAPAYA LEAF:

FTIR BEFORE SONICATION:

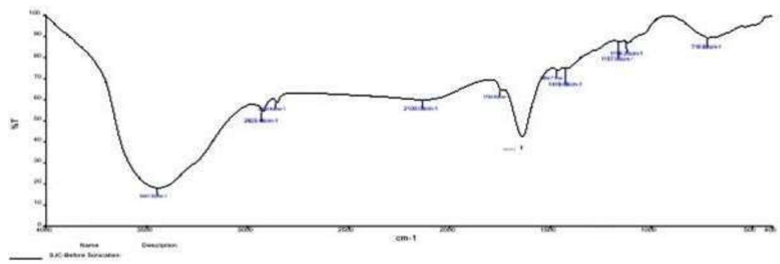

Graph.5.6.1.1

FTIR AFTER SONICATION

FTIR AFTER SONICATION (5 MINUTES):
(15 MINUTES):

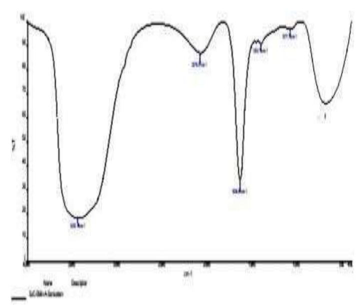

Graph.5.6.1.2

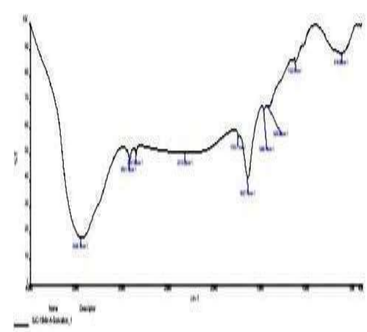

Graph.5.6.1.3

5.6.2. MORINGA OLEIFERA LEAF:

FTIR BEFORE SONICATION:

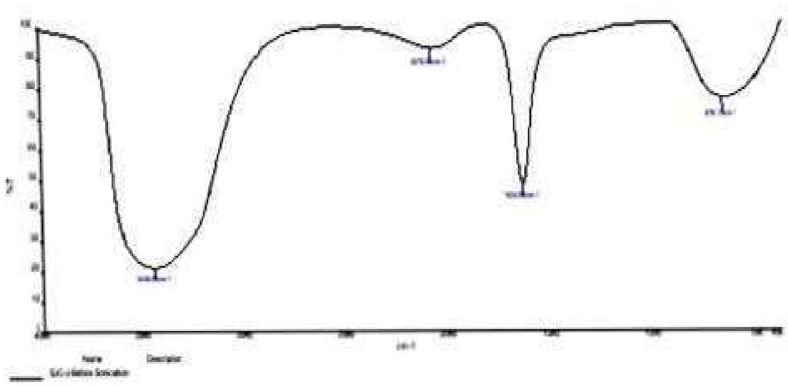

Graph.5.6.2.1

FTIR AFTER SONICATION

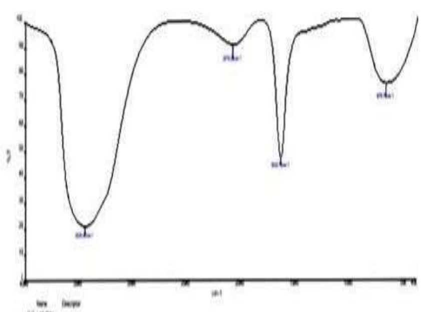

Graph.5.6.2.2

FTIR AFTER SONICATION (5 MINUTES):
(15 MINUTES):

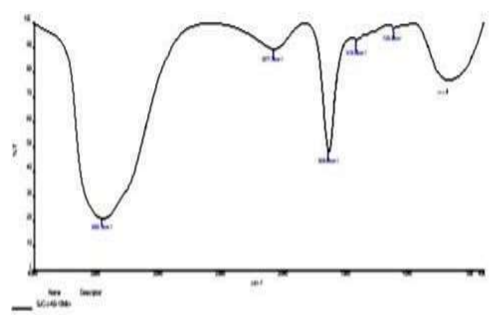

Graph.5.6.2.3

FOURIER TRANSFORM INFRARED SPECTROSCOPY: CARICA PAPAYA LEAF:
FTIR BEFORE SONICATION:

WAVENUMBER cm^-1	FUNCTIONAL GROUP
3441.52	O-H (Hydroxyl)
2923.46	C-H (Carbon-Hydrogen)
2853.64	C-H (Carbon-Hydrogen)
2130.09	C≡ C (Alkynes)
1742.64	C=O (Carbonyl)
1638.43	C=C (Alkenes)
1464.71	CH2 Group in Alkanes
1418.68	CH2 Group in Alkanes
1157.90	C-O-C Ether
1118.23	C-O-C (Carbonyl- Hydrogen
718.82	(C-Cl)

Table.5.6.1.1

CARICA PAPAYA LEAF:

FTIR AFTER SONICATION (5 MINUTES):

WAVENUMBER cm^-1	FUNCTIONAL GROUP
3435.15	O-H (Hydroxyl)
2078.57	C≡ N (Nitrile)
1636.61	C=C (Alkene)
1404.78	CH3 (Methyl)
1077.78	C-O (Carbon –Oygen)
686.77	C-H (Carbon –Hydrogen)

Table.5.6.1.2

CARICA PAPAYA LEAF:

FTIR AFTER SONICATION (15 MINUTES):

WAVENUMBER cm^-1	FUNCTIONAL GROUP
3448.10	O-H (Hydroxyl)
2921.72	C-H (Carbon-Hydrogen)
2851.83	C-H (Carbon-Hydrogen)
2313.08	CO2
1743.71	C=0 (Carbonyl)
1637.78	C-=c (Alkane)
1466.73	CH2 Groups in Alkanes
1420.88	CH2 Groups in Alkanes
1122.01	C-O Carbon Oxygen
616.88	C-Br Carbon Bromide

Table.5.6.1.3

FOURIER TRANSFORMS INFRARED SPECTROSCOPY: MORINGA OLEIFERA LEAF:
FTIR BEFORE SONICATION:

WAVENUMBER (cm^-1)	FUNCTIONAL GROUP
3441.52	O-H Group (Hydroxyl Groups OH)
2923.46	C-H bonds in Alkanes
2853.64	C-H bonds in Alkanes
2130.09	C≡ C (Alkynes)
1742.64	C=O (Carbonyl Group)
1638.43	C=O (Carbonyl Group)
1464.71	Methylene (CH2) Groups in Alkanes,Alkenes and Alkynes
1418.68	Methyl (CH3) Group
1157.9	C-O bonds in ether (R-O-R)
1118.23	C-O bonds in esters
718.82	C-H bonds in Benzene rings

Table.5.6.2.1

MORINGA OLEIFERA LEAF:
FTIR AFTER SONICATION (5 MINUTES):

WAVENUMBER (cm^-1)	FUNCTIONAL GROUP
3435.15	0-H Bonds in Alcohols and Phenols
2078.57	C≡ N (Nitrile)
1636.61	C=O Carbonyl Group In Amides
1404.78	Methyl (CH3) Group in Alkanes
1077.78	C-O Bonds in ethers
686.77	C-H Bonds in Benzene rings

Table.5.6.2.2

MORINGA OLEIFERA LEAF:

FTIR AFTER SONICATION (15 MINUTES):

WAVENUMBER cm^-1	FUNCTIONAL GROUP
3448.10	O-H Bonds in Alcohols and Benzenes
2921.72	C-H Bonds in Alkanes, Alkenes and Alkynes
2851.83	C-H Bonds in Alkanes, Alkenes and Alkynes
2313.08	C≡ C (Alkynes)
1743.71	C=O Carbonyl Group
1637.78	C=O Carbonyl Group
1466.73	CH2 Group
1420.88	Methyl CH3 Group
1122.01	C-O Bond in Ether
616.88	C-H Bond in Benzene Rings

Table.5.6.2.3

FTIR ANANYSIS:

- FTIR analysis of both Carica Papaya and MoringaOleifera leaves were taken; the difference between sonication for 5 minutes and 15 minutes could lead to the formation or breakdown of different functional groups.
- In Carica Papaya samples ,after sonication (5 minutes) the weakly bonded was broken, such as C-H (Carbon Hydryl),C-O (Carbon Hydrogen) and CH2 group in alkanes in before sonication was broken into CH (Carbon Hydrogen) and after sonication(15 minutes) the new functional groups were formed such as C-Br (Carbon Bromine).
- In MoringsOleifera samples ,after sonication (5 minutes) the weakly bonded was broken, such as C-H (Carbon Hydryl),C-O (Carbon Hydrogen) and CH2 group in alkanes in before sonication was broken into CH bonds in benzene rings and after sonication(15 minutes) the new functional groups were formed such as CH3 (Methyl group) and C-O bond in ether.

5.7 ANTIMICROBIAL OAD:

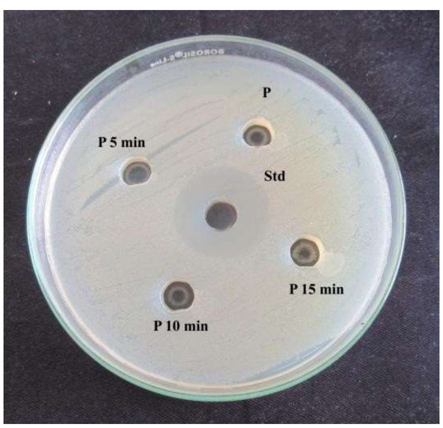

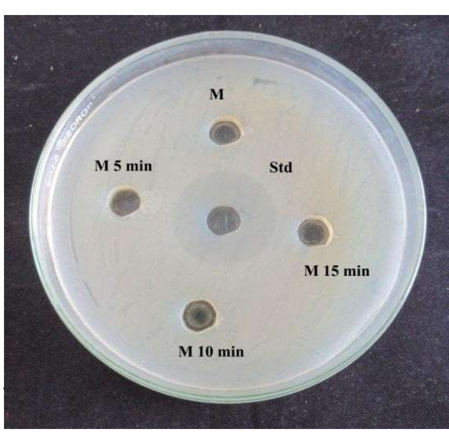

Fig.5.7.1.CARICA PAPAYA LEAF

SAMPLE CONCENTRATION	ZONE OF INHIBITION (nm)	ZONE OF INHIBITION (nm)
	ENTEROCOCCUS FAECALIS	PSEUDOMONAS AERUGINOSA
PAPAYA LEAF(BEFORE SONICATION)		

PAPAYA LEAF (AFTER SONICATION 5MINUTUES)		
PAPAYA LEAF (AFTER SONICATION 10 MINUTUES)		
PAPAYA LEAF (AFTER SONICATION 15 MINUTUES)		

MORINGA OLEIFERA LEAF (BEFORE SONICATION)		
MORINGA OLEIFERA LEA		

F (AFTER SONICATION 5 MINUTES)		
MORINGA OLEIFERA LEAF (AFTER SO		

NICATION 10 MINUTES)		
MORINGA OLEIFERA LEAF (AFTER SONICATION 1		

5 MINUTES		

Table.5.7

5.8 CONCLUSION:

- The Physical Parameters such as Density, Viscosity, Ultrasonic Velocity Adiabatic Compressibility and Acoustic Impedance were calculated before and after sonication and observed the changes.
- The Protein and Carbohydrate estimation of Carica Papaya and Moringa Oleifera Leaves before sonication and after sonication for the time intervals of 5 minutes and 15 minutes was observed and it confirms that there is an gradual increasing in the estimation of Protein and Carbohydrate after sonication.
- In FTIR and UV analysis of both samples before and after sonication found that changes occurred in peak intensities and functional groups ,shows that cell disruption occurred in the samples.
- The reduction in particle size of both samples after sonication attributed to shear forces, cavitation and enhanced mass transfer.
- In Antimicrobial Load for the Papaya Leaf sample before sonication in Enterococcus Faecalis has 12 nm zone of inhibition was observed while for the after sonication of time intervals of 5 ,10 and 15 minutes and in Pseudmonas aeruginosa has null effect .For the sample Moringa Oleifera Leaf before and after sonication of time intervals 5,10 and 15 minutes was totally in null effect in both Enterococcus Faecalis and Pseudomonas aeruginosa .

3.1 Particle Size Analyzer

Particle size analyzers are essential tools for determining the size and distribution of particles within a material. These analyzers find applications in various fields, including research and development, manufacturing, quality control, and product testing. Different technologies allow analysis across a wide range of particle sizes in various forms—powder, liquid, or aerosol—covering diverse materials, from soil to paint and cosmetics. Laser diffraction particle size analyzers calculate particle sizes based on the angle of scattered light as particles pass through a laser beam. **Fig.3** illustrates particle size analysis of carica papaya leaf and **Fig.4** illustrates the particle size analysis of moringa oleifera leaf:

This continuous measurement technique can analyze bulk material across a size range of 10 nm to 3 mm. The sensitivity and size limits of a laser diffraction analyzer depend on the number and placement of detectors. In contrast, dynamic light scattering determines size from fluctuations in scattered laser light intensity caused by Brownian motion of the particles. Additionally, induced grating particle size analyzers can identify smaller particles (0.5 nm to 200 nm) in solutions by electrically aligning particles and measuring their diffusion.

Particle size and distribution significantly influence material properties, including reaction rate**;** for solids, the surface area of the particle plays a critical role in determining the rate of chemical reactions. Chemical reactions occur more readily in fine particles. For instance, the cement industry relies on appropriate reaction rates to achieve products with desired strengths. Dissolution rate is also affected by particle size. Finer particles have a larger surface area, which reduces physical barriers to dissolution, enabling faster processes. This characteristic is crucial in the pharmaceutical industry, where the speed of dissolution directly impacts drug bioavailability and effectiveness. Packing density, or the efficiency of how particles pack together, is another critical factor in various industries. Larger particles typically pack less efficiently than smaller ones. Reducing particle size improves packing density and reduces voidage (unoccupied volume), which is vital in metal and ceramic production through mold filling, as unoccupied volume can lead to flawed products. Product appearance is influenced by particle size as well. In the manufacture of paints, inks, toners, and surface coatings, the way particles scatter light determines various parameters, including hue, tint, and transparency.

3.2 FTIR analysis

Fourier Transform Infrared Spectroscopy (FT-IR) is a widely used analytical technique for identifying and quantifying materials based on their unique infrared absorption spectra. In this study, FT-IR was employed to investigate the molecular changes in the leaves of Carica Papaya (**Fig.5)** and Moringa Oleifera (**Fig.6)** resulting from sonication times of 5 minutes and 15 minutes. The analysis revealed that sonication for 5 minutes in Carica Papaya led to the breaking of weak bonds, such as C-H (Carbon-Hydrogen), C-O (Carbon-Oxygen), and CH_2 groups in alkanes. Following this, sonication for 15 minutes resulted in the formation of new functional groups, including C-Br (Carbon-Bromine). Similarly, in Moringa Oleifera**,** sonication for 5 minutes also caused the breakdown of weakly bonded structures, including C-H and C-O groups. After 15 minutes of sonication, new functional groups such as CH_3 (Methyl group) and C-O bonds in ethers were identified. This analysis highlights the influence of sonication time on the functional group composition of both plant leaves. **Table 3** lists the FTIR analysis of Carica papaya leaf and **Table 4** lists the FTIR analysis of Moringa Oleifera leaf**.**

3.3 Ultraviolet Spectroscopy

The ultraviolet (UV) spectroscopy analysis of *Carica papaya* leaf extracts was performed to investigate the absorption characteristics and changes induced by sonication. The UV-Vis spectra (**Fig. 7.**) revealed prominent absorption peaks in the UV region, indicating the presence of bioactive compounds such as alkaloids, phenolics, and flavonoids. The spectrum prior to sonication displayed distinct peaks, which showed notable shifts and variations in intensity following 5 and 15 minutes of sonication. These changes suggest that sonication facilitates the breakdown of cellular structures, leading to enhanced release and extraction of phytochemicals. This highlights the effectiveness of sonication in improving the yield and availability of bioactive compounds from *Carica papaya* leaves, making it a valuable technique for phytochemical extraction.

The ultraviolet (UV) spectroscopy analysis of *Moringa oleifera* leaf extracts was conducted to evaluate changes in absorption profiles before and after sonication. The UV-Vis spectra (**Fig. 8)** exhibited characteristic absorption peaks in the UV region, indicating the presence of biomolecules such as phenolics and flavonoids. Prior to sonication, distinct absorption peaks were observed at specific wavelengths, which showed slight shifts and variations in intensity after 5 and 15 minutes of sonication. These changes suggest a potential alteration in the molecular structure or the release of bioactive compounds due to the sonication process. The observed spectral variations confirm that sonication enhances the extraction efficiency, potentially improving the bioavailability of active compounds in the leaf extract. These findings underline the significance of sonication as a preparatory technique in optimizing the extraction of phytochemicals from *Moringa oleifera* leaves.

3.4 Protein and Carbohydrate Estimation

Proteins are essential macronutrients crucial for various bodily functions, including muscle repair, enzyme production, and immune function. Estimating protein intake is vital for individuals seeking to optimize their nutrition, support muscle development, and maintain overall health. This process involves determining the protein content in foods and beverages, enabling informed dietary choices and meeting protein needs effectively. For athletes aiming to maximize muscle gains, individuals managing dietary restrictions, or anyone striving for a balanced diet, understanding protein content is key to achieving nutritional goals. This guide explores methods for estimating protein content in both animal and plant-based foods, discussing the importance of protein in the diet, its role in health and performance, and practical tips for accurate estimation. Resources and tools for tracking protein intake will also be highlighted.

Mastering protein estimation enhances nutritional awareness, facilitates better dietary choices, and unlocks the benefits of a protein-rich diet for improved health and well-being. Estimating protein intake ensures individuals consume sufficient amounts of this essential nutrient, critical for the growth, repair, and maintenance of body tissues. By estimating protein intake, individuals can assess whether they meet daily requirements for optimal health. Protein is particularly important for those engaged in physical activity. Estimating protein intake helps optimize muscle health and development by providing sufficient amino acids for muscle repair and growth, which is essential for maximizing exercise-induced muscle adaptations and overall athletic performance.

The protein estimation of *Carica papaya* and *Moringa oleifera* leaf extracts (**Table 5)** was conducted to assess the effect of sonication on protein release. Before sonication, the protein content in *Carica papaya* leaf extract was 300 µg, while *Moringa oleifera* leaf extract exhibited a higher protein content of 610 µg. After 5 minutes of sonication, the protein content increased to 330 µg and 630 µg, respectively. A significant enhancement was observed after 15 minutes of sonication, with *Carica papaya* reaching 440 µg and *Moringa oleifera* reaching 740 µg. These results indicate that sonication effectively disrupts cell structures, facilitating the release of proteins and enhancing extraction efficiency, particularly in *Moringa oleifera* leaves.

Carbohydrate estimation plays a vital role in human nutrition, serving as the primary energy source for the body. It is particularly essential for individuals managing health conditions like diabetes, as accurate estimation of carbohydrate intake helps in making informed dietary choices. This estimation process not only involves counting grams of sugar or starch but also understanding the composition of complex carbohydrates, fiber, and sugars in various foods. By estimating carbohydrate content, individuals can tailor their food choices to maintain stable blood sugar levels and overall health.

Carbohydrate estimation also plays a crucial role in sports nutrition and weight management. Athletes rely on carbohydrates for energy during workouts and competitions, making accurate estimation vital for optimizing performance. Similarly, those managing their weight can benefit from understanding the carbohydrate content of foods, allowing them to make choices aligned with their calorie and nutrition goals. The process of carbohydrate estimation encompasses various methods for estimating carbohydrates in both solid and liquid foods, providing practical tips for accurate assessment and highlighting resources for further information. Overall, mastering carbohydrate estimation empowers individuals to take control of their nutrition, promote better health outcomes, and achieve their dietary objectives effectively.

The carbohydrate estimation of *Carica papaya* and *Moringa oleifera* leaf extracts (**Table 6)** was performed to analyze the impact of sonication on carbohydrate release. Before sonication, the carbohydrate content was measured at 170 µg in *Carica papaya* leaves and 280 µg in *Moringa oleifera* leaves. After 5 minutes of sonication, the carbohydrate content increased to 200 µg in *Carica papaya* but slightly decreased to 270 µg in *Moringa oleifera*. A substantial increase was observed after 15 minutes of sonication, with *Carica papaya* reaching 340 µg, while *Moringa oleifera* exhibited a slight rise to 300 µg. These findings suggest that sonication significantly enhances carbohydrate release in *Carica papaya*, while its effect on *Moringa oleifera* is comparatively moderate.

3.5 Antimicrobial Activity Assessment

The assessment of antimicrobial load in the context of sonication is crucial for understanding its efficacy in reducing microbial contamination or biofilm formation. Sonication involves using sound waves to agitate a solution, disrupting microbial cells or biofilms and enhancing the effectiveness of antimicrobial treatments. This method facilitates the penetration of antimicrobial agents into microbial cells or biofilms by disrupting their structure, allowing for higher proportions of microbial cells to be reached and killed by the treatment.

Additionally, biofilms, which are complex communities of microorganisms resistant to antimicrobial agents, can be disrupted by sonication. Evaluating the antimicrobial load before and after sonication provides insights into the extent of biofilm disruption and the subsequent reduction in microbial viability. In clinical and laboratory settings, sonication is often part of cleaning and decontamination procedures for medical instruments and laboratory glassware. Assessing antimicrobial load helps validate the effectiveness of these cleaning protocols by confirming the reduction in microbial contamination following sonication treatment. Moreover, in microbiological research, sonication is sometimes employed to study antimicrobial resistance mechanisms or to extract microbial DNA or proteins. By quantifying the impact of sonication on microbial viability or susceptibility to antimicrobial agents, researchers and clinicians can make informed decisions about the use of sonication in various applications.

The antimicrobial activity of the samples were determined by the well diffusion method on Muller Hinton Agar (MHA) medium. **Fig. 9**. Antimicrobial activity analyses Carica papaya leaf and moringa oleifera leaf. To prepare the MHA, 3.8 grams of the medium were dissolved in 100 mL of distilled water, along with 1 gram of agar. This mixture was then sterilized. After sterilization, the medium was poured into sterile petri plates and allowed to solidify for 1 hour. Once solidified, the inoculum was spread evenly on the solid plates using a sterile swab moistened with the bacterial suspension. Wells were created in the agar using a cork borer. Samples (60 µL) and the positive control, Streptomycin (1 mg/mL - 20 µL), were loaded into the respective wells. The plates were incubated for 24 hours at 37ºC. After incubation, microbial growth was assessed by measuring the diameter of the zone of inhibition.

3.6 Bacterial Characteristics:

3.6.1 Enterococcus faecalis:

Enterococcus faecalis is a Gram-positive bacterium commonly found in the gastrointestinal tracts of humans and animals. While it is typically a commensal organism, it can also act as an opportunistic pathogen, causing infections such as urinary tract infections, bacteremia, and endocarditis. In terms of antimicrobial activity, Enterococcus faecalis may exhibit resistance to various antibiotics, including penicillins and aminoglycosides. Its role in antimicrobial activity can be twofold: first, resistant strains can serve as indicators for the prevalence and spread of antibiotic resistance in environments like healthcare settings. Second, some strains of Enterococcus faecalis are known to produce antimicrobial compounds, such as bacteriocins, which inhibit the growth of other bacteria and may have applications in probiotics or food preservation.

3.6.2 Pseudomonas aeruginosa:

Pseudomonas aeruginosa is a Gram-negative bacterium recognized for its versatile metabolic capabilities and its ability to thrive in diverse environments, including soil, water, and human tissues. This opportunistic pathogen is associated with various infections, particularly in immunocompromised individuals or those with cystic fibrosis, burns, or wounds. Pseudomonas aeruginosa exhibits intrinsic resistance to many antibiotics due to its impermeable outer membrane and efflux pump systems, making infections challenging to treat. Nonetheless, it plays a significant role in antimicrobial activity by producing a wide array of secondary metabolites, including antimicrobial compounds such as pyocyanin, pyoverdine, and pyrrolnitrin, which can inhibit the growth of competing microorganisms. In certain contexts, specific strains of Pseudomonas aeruginosa have been explored as biocontrol agents against plant pathogens and in bioremediation efforts due to their ability to produce antimicrobial compounds that target other microorganisms.

4. CONCLUSION

The study evaluated several physical parameters, including density, viscosity, ultrasonic velocity, adiabatic compressibility, and acoustic impedance, before and after sonication, revealing notable changes. Protein and carbohydrate estimations of *Carica Papaya* and *Moringa Oleifera* leaves demonstrated a gradual increase in both macromolecules following sonication at intervals of 5 and 15 minutes. FTIR and UV analyses indicated changes in peak intensities and functional groups, confirming cell disruption in the samples. The reduction in particle size for both samples post-sonication was attributed to shear forces, cavitation, and enhanced mass transfer. In terms of antimicrobial activity, the *Carica Papaya* leaf sample exhibited a 12 mm zone of inhibition against *Enterococcus faecalis* before sonication, with no effect observed against *Pseudomonas aeruginosa* across all sonication time intervals (5, 10, and 15 minutes). Conversely, *Moringa Oleifera* leaves showed no antimicrobial activity against either *Enterococcus faecalis* or *Pseudomonas aeruginosa* before and after sonication at the specified intervals.

Acknowledgments

The author Dr.G.Samuel thanks the management of St. Joseph's College, Tiruchirappalli for funding to complete this work through **SJCRG** (St. Joseph's College Research Grant) (Autonomous), Tiruchirappalli-02.

Conflict of Interest Statement

The authors state no conflict of interest.

Data Availability Statement

On reasonable request, the corresponding author will make the whole datasets created and/or analyzed during the current work available

Ethical Approval Statement:

This study did not require approval from an ethics committee, as it does not involve human participants, animals, or sensitive data requiring ethical clearance. All research was conducted in accordance with applicable ethical guidelines.

Authors Contribution

G. Samuel: The conception and design of the study, or acquisition of data. Analysis and interpretation of data.

K. Srijanani: Drafting the article or revising it critically for important intellectual content.

I. Johnson: Final approval of the version to be submitted.

References:

[1] Prusty, D., Gallegos, A., & Wu, J. (2024). Unveiling the Role of Electrostatic Forces on Attraction between Opposing Polyelectrolyte Brushes. *Langmuir*, *40*(4), 2064-2078

[2] Riera, M., Talbot, J. J., Steele, R. P., & Paesani, F. (2020). Infrared signatures of isomer selectivity and symmetry breaking in the Cs+ (H2O) 3 complex using many-body potential energy functions. *The Journal of Chemical Physics*, *153*(4).

[3] Horstmann, R., Hecht, L., Kloth, S., & Vogel, M. (2022). Structural and dynamical properties of liquids in confinements: A review of molecular dynamics simulation studies. *Langmuir*, *38*(21), 6506-6522.

[4] Ulusoy, U. (2023). A review of particle shape effects on material properties for various engineering applications: from macro to nanoscale. *Minerals*, *13*(1), 91.

[5] Tanasheva, N. K., Dyusembaeva, A. N., Bakhtybekova, A. R., Minkov, L. L., Burkov, M. A., Shuyushbayeva, N. N., & Tleubergenova, A. Z. (2024). CFD simulation and experimental investigation of a Magnus wind turbine with an improved blade shape. *Renewable Energy*, *237*, 121698.

[6] Zelenski, M., Simakin, A., Taran, Y., Kamenetsky, V. S., & Malik, N. J. G. E. C. A. (2021). Partitioning of elements between high-temperature, low-density aqueous fluid and silicate melt as derived from volcanic gas geochemistry. *Geochimica et*

Cosmochimica Acta, *295*, 112-134.

[7] Zhang, D., Ronson, T. K., Zou, Y. Q., & Nitschke, J. R. (2021). Metal–organic cages for molecular separations. *Nature Reviews Chemistry*, *5*(3), 168-182.

[8] Špadina, M., Dufrêche, J. F., Pellet-Rostaing, S., Marčelja, S., & Zemb, T. (2021). Molecular forces in liquid–liquid extraction. *Langmuir*, *37*(36), 10637-10656.

[9] Moradpour, N., Yang, J., & Tsai, P. A. (2024). Liquid foam: Fundamentals, rheology, and applications of foam displacement in porous structures. *Current Opinion in Colloid & Interface Science*, 101845.

[10] Gao, S., Yang, Y., Falchevskaya, A. S., Vinogradov, V. V., Yuan, B., Liu, J., & Sun, X. (2024). Phase transition liquid metal enabled emerging biomedical technologies and applications. *Advanced Science*, *11*(37), 2306692.

11] Lee, W. T. C., Yin, Y., Morten, M. J., Tonzi, P., Gwo, P. P., Odermatt, D. C., ... & Rothenberg, E. (2021). Single-molecule imaging reveals replication fork coupled formation of G-quadruplex structures hinders local replication stress signaling. *Nature communications*, *12*(1), 2525.

[12] Saini, A., Prabhune, A., Mishra, A. P., & Dey, R. (2021). Density, ultrasonic velocity, viscosity, refractive index and surface tension of aqueous choline chloride with electrolyte solutions. *Journal of Molecular Liquids*, *323*, 114593.

[13] Vogel, S. (2020). *Life in moving fluids: the physical biology of flow-revised and expanded second edition*. Princeton university press.

[14] Hertzberg, R. W., Vinci, R. P., & Hertzberg, J. L. (2020). *Deformation and fracture mechanics of engineering materials*. John Wiley & Sons.

[15] Fu, W., Yan, X., Gurumukhi, Y., Garimella, V. S., King, W. P., & Miljkovic, N. (2022). High power and energy density dynamic phase change materials using pressure-enhanced close contact melting. *Nature Energy*, *7*(3), 270-280.

[16] Manickam, S., Boffito, D. C., Flores, E. M., Leveque, J. M., Pflieger, R., Pollet, B. G., & Ashokkumar, M. (2023). Ultrasonics and sonochemistry: Editors' perspective. *Ultrasonics Sonochemistry*, *99*, 106540.

[17] Hahmann, J., Ishaqat, A., Lammers, T., & Herrmann, A. (2024). Sonogenetics for Monitoring and Modulating Biomolecular Function by Ultrasound. *Angewandte Chemie International Edition*, *63*(13), e202317112.

[18] Li, X., Porcino, M., Martineau-Corcos, C., Guo, T., Xiong, T., Zhu, W., ... & Gref, R. (2020). Efficient incorporation and protection of lansoprazole in cyclodextrin metal-organic frameworks. *International Journal of Pharmaceutics*, *585*, 119442.

[19] Fan, J., & Wang, F. (2021). Review of ultrasonic measurement methods for two-phase flow. *Review of Scientific Instruments*, *92*(9).

[20] Das, N., Praharaj, M. K., & Panda, S. (2024). Exploring ultrasonic wave transmission in liquids and liquid mixtures: A comprehensive overview. *Journal of Molecular Liquids*, 124841.